Persistent Electrical Coupling and Locomotory Dysfunction in the Zebrafish Mutant *shocked*

Victor M. Luna, Meng Wang, Fumihito Ono, Michelle R. Gleason, Julia E. Dallman, Gail Mandel and Paul Brehm

J Neurophysiol 92:2003-2009, 2004. First published 16 June 2004; doi:10.1152/jn.00454.2004

Journal of Neurophysiology publishes original articles on the function of the nervous system. It is published 12 times a year (monthly) by the American Physiological Society, 9650 Rockville Pike, Bethesda MD 20814-3991. ISSN: 0022-3077, ESSN: 1522-1598. Visit our website at http://www.the-aps.org/.

J Neurophysiol 92: 2003–2009, 2004.
First published June 16, 2004; 10.1152/jn.00454.2004.

Persistent Electrical Coupling and Locomotory Dysfunction in the Zebrafish Mutant *shocked*

Victor M. Luna,[1]* Meng Wang,[1]* Fumihito Ono,[1] Michelle R. Gleason,[1,2] Julia E. Dallman,[1] Gail Mandel,[1,2] and Paul Brehm[1]

[1]*Department of Neurobiology and Behavior and* [2]*Howard Hughes Medical Institute, State University of New York, Stony Brook, New York 11794*

Submitted 3 May 2004; accepted in final form 8 June 2004

Luna, Victor M., Meng Wang, Fumihito Ono, Michelle R. Gleason, Julia E. Dallman, Gail Mandel, and Paul Brehm. Persistent electrical coupling and locomotory dysfunction in the zebrafish mutant *shocked*. *J Neurophysiol* 92: 2003–2009, 2004. First published June 16, 2004; 10.1152/jn.00454.2004. On initial formation of neuromuscular junctions, slow synaptic signals interact through an electrically coupled network of muscle cells. After the developmental onset of muscle excitability and the transition to fast synaptic responses, electrical coupling diminishes. No studies have revealed the functional importance of the electrical coupling or its precisely timed loss during development. In the mutant zebrafish *shocked* (*sho*) electrical coupling between fast muscle cells persists beyond the time that it would normally disappear in wild-type fish. Recordings from *sho* indicate that muscle depolarization in response to motor neuron stimulation remains slow due to the low-pass filter characteristics of the coupled network of muscle cells. Our findings suggest that the resultant prolonged muscle depolarizations contribute to the premature termination of swimming in *sho* and the delayed acquisition of the normally rapid touch-triggered movements. Thus the benefits of gap junctions during early synapse development likely become a liability if not inactivated by the time that muscle would normally achieve fast autonomous function.

INTRODUCTION

Since their initial discovery, gap junctions have been found to play important physiological roles in nearly all types of tissues (Harris 2001). A notable exception is adult vertebrate skeletal muscle that lacks electrical coupling. During early development, however, it appears that most, if not all vertebrate skeletal muscle, exhibits extensive electrical coupling (Armstrong et al. 1983; Balogh et al. 1993; Buss and Drapeau 2000; Schmalbruch 1982). The function of this intercellular communication is likely to involve strengthening of immature synaptic responses via distribution of synaptic currents among muscle (Buss and Drapeau 2000). On initial formation, neuromuscular synapses are weak due to ineffective transmitter release and incompletely developed postsynaptic receptor machinery. To counter these limitations, depolarization is maximized by expression of embryonic isoforms of postsynaptic receptors with slow kinetics (Jaramillo et al. 1988). Another potential mechanism for strengthening synaptic responses is electrical coupling, which can provide both temporal and spatial summation. Interestingly, the electrical coupling in frog muscle is lost after the transition to fast synaptic mechanisms (Armstrong et al. 1983; Brehm et al. 1984). Thus the timed loss of electrical coupling likely plays an important role in fostering the further functional development of skeletal muscle or neuromuscular transmission. However, no published studies on muscle have shed light on this interesting issue.

In the course of analyzing mutant zebrafish, we have identified a line that has provided new insights into the role of gap junctional coupling in skeletal muscle. Within 3 days after fertilization, wild-type zebrafish acquire the ability to swim rapidly in response to touch. At the same age, we find that mutant *shocked* (*sho*) fish exhibit a profound locomotory defect that is reflected in an aborted escape response (Granato et al. 1996). Our physiological analyses have revealed an unusual persistence of extensive coupling in *sho* fish that may contribute to the motility phenotype. However, the mutation responsible for excessive coupling does not reside in the gene encoding connexin 43, the predominant gap junctional isoform in skeletal muscle (Balogh et al. 1993).

METHODS

The mutant line of zebrafish *sho te*^{301} was obtained from the Max-Planck Institute (Granato et al. 1996). Adult fish heterozygous for the *sho* mutation were crossed to generate homozygous embryos used for this study.

Whole cell patch clamp recordings were performed on tail muscle of in vivo fish. For this purpose, the fish were decapitated, skinned, and immobilized on a silicone elastomer (Sylgard) substrate with tungsten pins. The recordings were performed on a Zeiss FS microscope using differential interference contrast and a ×40 water-immersion objective. These optics permitted unequivocal distinction between fast and slow muscle on the basis of the morphology and orientation (Lefevbre et al. 2004). The detailed methodology for recording of both spontaneous and evoked synaptic current is described elsewhere (Ono et al. 2001, 2002). For dual muscle recordings of coupling and spontaneous synaptic currents, a List EPC9/2 amplifier (Instrutech, Port Washington, NY) was used. An AM Systems 2100 stimulator (Carlsborg, WA) was used to stimulate the spinal cord. All data were obtained at 100-kHz sampling rate and filtered at 10 kHz for analysis. Analysis of data were performed using combinations of Igor (WaveMetrics, Lake Oswego, OR), MiniAnalysis (Synaptosoft, Decatur, GA), and HekaPulse Fit (Instrutech). Statistics were performed using the Student's *t*-test and the SDs along with the mean values are indicated. The whole cell internal recording solution contained (in mM) 120 KCl, 5 K-HEPES, and 5 BAPTA, and the bath solution contained (in mM) 110 NaCl, 5 Na-HEPES, 4 $CaCl_2$, 3

* V. M. Luna and M. Wang contributed equally to this work.

Address for reprint requests and other correspondence: P. Brehm, Dept. of Neurobiology and Behavior, State University of New York at Stony Brook, Stony Brook, NY 11794 (E-mail: pbrehm@notes.cc.sunysb.edu).

The costs of publication of this article were defrayed in part by the payment of page charges. The article must therefore be hereby marked "*advertisement*" in accordance with 18 U.S.C. Section 1734 solely to indicate this fact.

glucose, 2 KCl, and 1 $MgCl_2$. Recordings of fictive swimming motor patterns were made by placing a 10-μm-diam pipette in the myocommatal region and applying gentle suction (Masino and Fetcho 2003). Careful repositioning of the electrode provided optimal signal-noise for recording ventral root action currents. For these recordings, fish were not decapitated, but they were treated with 1 μM α-bungarotoxin to block contractions. The fictive swimming episodes were initiated by either shining a bright light in the eye or tapping the head.

18β-glycyrrhetinic acid (Sigma) was stored at room temperature as a 0.1 M stock solution in DMSO. Lucifer yellow (Sigma) was stored at 4°C in 0.1% internal whole cell recording solution.

Connexin 43 from *sho* fish was sequenced to identify mutations that may occur in the coding region. The coding region of connexin 43 occurs in a single exon, which was PCR amplified from genomic *sho* DNA using primers f-GCTAGAACTCCCTCAAGATGGG and r-TGTCAGTCCTCTAGCGTTGGG and sequenced. For mapping studies, genomic DNA was extracted from individual day 3 embryos by overnight incubation in 1.7 mg/ml proteinase K (Invitrogen) in 10 mM Tris pH 8.0 with 1 mM EDTA at 55°C. An equivalent amount of this preparation was taken from 20 fish and pooled for bulk segregant analysis (Postlethwait and Talbot 1997), which was performed with a set of 214 microsatellite markers (http://zebrafish.mgh.harvard.edu/) (Invitrogen, Carlsbad, CA).

RESULTS

The *sho* phenotype is first manifest in homozygous mutant fish at day 3 of development (Granato et al. 1996). At this stage, wild-type fish acquire the ability to swim rapidly away from a mechanical touch. In *sho* fish, however, a strong mechanical stimulus results in a single slow tail flip, followed by an abrupt termination of swimming (Fig. 1*A*). The delayed single contracture is a powerful and protracted bend, yielding the impression that the contraction itself contributes to cessation of swimming. *Sho* fish partially recover so that by day 6 most of the fish have acquired the ability to mount a reasonable escape response (Fig. 1*A*). The escape response in such fish is still, however, more difficult to elicit than those of wild-type fish. Despite the improved ability to swim the *sho* fish generally die within the first 2 wk.

To test whether defective swimming is reflected in altered motor patterns in day 3 *sho* fish, we first performed multiunit extracellular recordings from motor neuron ventral roots (Masino and Fetcho 2003). These recordings provide an indicator as to whether *sho* fish are able to generate the rhythmic CNS drive that underlies persistent swimming in wild-type fish. It was necessary to first paralyze these fish by treatment with α-bungarotoxin to prevent global muscle contractions. The fictive motor pattern was evoked either by tapping the fish on the head or shining light into the eyes. In every *sho* and wild-type fish tested, a patterned motor output was observed that lasted for several seconds (Fig. 1*B*). This "fictive swimming" pattern in the nervous system is responsible for driving a coordinated and persistent swimming response. Importantly, it occurred in *sho* fish despite the inability of this mutant to mount any lasting or coordinated swimming. Quantitative analyses of the patterned output indicated a mean burst interval of 51.2 $\pm$ 6.5 ms (n = 4) in *sho* fish that was not significantly different (P = 0.13) from 44.2 $\pm$ 5.4 ms (n = 5) obtained for wild-type fish. Subtle differences may have gone undetected due to the poor signal strength and our inability to determine the firing pattern of individual units with this technique. One clear difference between mutant and wild-type fish was reflected in the increased difficulty in eliciting the patterned motor output in *sho* fish, consistent with the higher threshold for eliciting movement. However, this feature does not explain the inability to swim in response to the patterned output. Therefore we turned our attention to electrophysiological recording from skeletal muscle to test for defects.

We next examined motor neuron-evoked muscle responses that might account for the abortive escape response in *sho*. For this purpose, we stimulated spinal motor neurons and recorded the associated synaptic current in fast muscle. Fast muscle was chosen because it is responsible for mediating the fast escape response that is largely defective in *sho* fish. Additionally, only fast muscle is able to generate action potentials in response to depolarization (Buss and Drapeau 2000). Voltage-clamp recordings from fast muscle of *sho* held at –50 mV showed a strongly biphasic decay (Fig. 2*A*). Exponential fitting of the current decay in *sho* muscle yielded a slow component that averaged 4.6 $\pm$ 1.2 ms (n = 8) and accounted for 34 $\pm$ 14% of the overall inward current, and a fast exponential component corresponding to 0.6 $\pm$ 0.2 ms (n = 8). Wild-type synaptic current decay was consistently fit with a single-exponential function that averaged 0.8 $\pm$ 0.1 ms (n = 21; Fig. 2*A*).

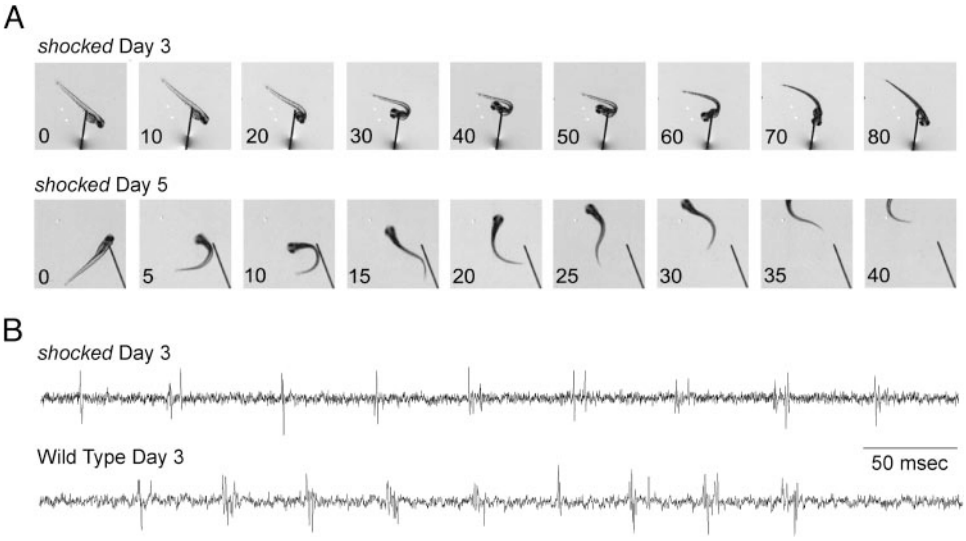

FIG. 1. Touch-mediated escape responses and the associated motor neuron outputs for *sho* vs. wild-type swimming. *A*: at time 0, an escape response was elicited by a gentle touch to the head. The time (in ms) after touch is shown for 3 day *sho* (*top*) and recovered 5 day *sho* (*bottom*) fish. *B*: extracellular recordings from ventral roots of 3 day *sho* (*top*) and wild-type (*bottom*) fish. This "fictive swimming" output was triggered by shining bright light into the eye of each fish.

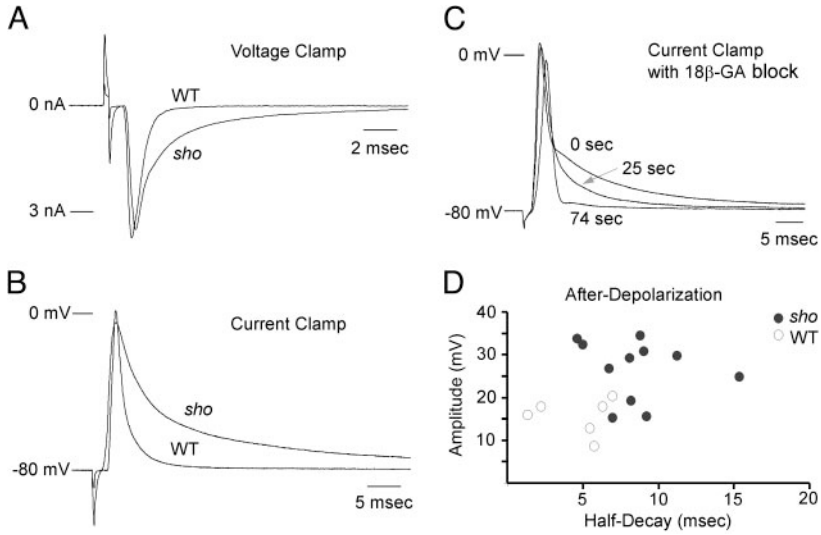

FIG. 2. Evoked action potentials and synaptic currents from fast skeletal muscle of day 3 wild-type and *sho* fish. *A*: stimulus-evoked synaptic currents recorded from voltage-clamped fast muscle of wild-type and *sho* fish. The membrane potential was held at –50 mV while the spinal motor neurons were extracellularly stimulated. *B*: representative stimulus-evoked endplate potentials from fast muscle of wild-type and *sho* fish. The stimulus artifact indicates the time at which the spinal cord was stimulated and the muscle membrane potential was −80 mV in both cells. *C*: time-dependent blockade of the stimulus-evoked afterdepolarization in fast muscle of *sho* fish after application of 75 μM 18 β-glycyrrhetinic acid. *D*: amplitude vs. half decay time are plotted for the stimulus-evoked endplate potential afterdepolarization in wild-type (○) and *sho* fish (●).

To examine the potential consequences of this exaggerated slow component of evoked postsynaptic current decay in *sho* muscle, we recorded using current-clamp methodology. The membrane was adjusted to approximately −80 mV, and the spinal neurons were stimulated extracellularly. In both wild-type and *sho* fish, a large fast rising muscle action potential was observed (Fig. 2*B*). Repolarization was accompanied by an afterdepolarization that was larger and slower in muscle of *sho* fish (Fig. 2, *B* and *D*). This afterdepolarization is probably a manifestation of the slow component of inward current decay that was observed under voltage clamp (Fig. 2*A*). It is also possible that the slowed repolarization could reflect differences in time constants for membrane charging that result from differences in input resistance. However, comparisons of input resistance indicated no significance difference ($P = 0.69$) between *sho* ($n = 9$; 49.3 ± 24.5 MΩ) and wild-type ($n = 9$; 55.2 ± 35.3 MΩ). More importantly, the fact that different current trajectories are observed for *sho* and wild-type fish under voltage clamp argue that differences in passive membrane properties are not solely responsible for slowed repolarization. This additional slow component of current decay in *sho* reflected either direct differences in synaptic current kinetics or differences in electrotonically transmitted synaptic currents between muscle cells (Nguyen et al. 1999). To determine whether this persistent current and associated afterdepolarization in *sho* fish originated from electrotonic currents through gap junctions, we applied 75 μM 18β-glycyrrhetinic acid to block electrical coupling (Fig. 2*C*). This compound effectively blocks electrical coupling in skeletal muscle (Proulx et al. 1997). On application, the afterdepolarization showed a time-dependent reduction in amplitude. This afterdepolarization decreased by 85% in response to the blocker indicating that this component was generated in neighboring muscle cells and reflected the summation of currents from those cells. In some cases, the block resulted in a small decrease in peak amplitude and a slight slowing of rise. This occurs despite the increase in input resistance that results from network uncoupling. It likely reflects a loss of synaptic current that is normally provided by electrical coupling with neighboring muscle. The decrease in early synaptic current would be expected to decrease the amount of depolarizing drive to the muscle.

We next examined spontaneous synaptic currents to determine whether the *sho* phenotype involved altered ACh receptor function. This approach has resulted in identification of several mutant lines of zebrafish wherein receptor function is altered (Lefevbre et al. 2004; Ono et al. 2001, 2002). As found for wild-type fish, whole cell recordings from skeletal muscle of *sho* fish reveal two separate classes of spontaneous synaptic events (Buss and Drapeau 2000) that can be readily separated on the bases of either rise time or decay kinetics (Fig. 3*A*). The fast class of events is generally much larger in amplitude than the slow class of events. The slow class of synaptic currents is consistently smaller than 60 pA and likely represents electrotonic reflections of currents actively generated in neighboring muscle (Buss and Drapeau 2000). Direct evidence that the small-amplitude class represents an electrotonic reflection of currents from nearby muscle is shown by the ability of 18β-glycyrrhetinic acid to eliminate these currents (Fig. 3*C*). This concentration of blocker increased the input resistance of fast muscle from 55 ± 35 ($n = 9$) to 272 ± 94 MΩ ($n = 5$), indicating a significant reduction in electrical coupling ($P < .001$). Additionally, transfer of Lucifer yellow between muscle cells was blocked in the presence of 75 μM 18β-glycyrrhetinic acid, further indicating a reduction in electrical coupling. Our measurements indicate that dye coupling spreads to 3.3 ± 1.2 fast muscle cells ($n = 9$) in 3-day fish, but no dye spread to neighboring cells was observed in the presence of blocker ($n = 5$). The larger-amplitude synaptic currents with fast rise times and decay times <1 ms remained in the presence of 75 μM 18β-glycyrrhetinic acid, indicating that they are generated directly by the muscle cell under whole cell voltage clamp. Examination of *sho* fish indicated a similar dual class of spontaneous synaptic currents (Fig. 3*B*). Quantitative comparisons between fast muscle of *sho* and wild-type revealed no significant differences for either the large fast class or small slow class. As with wild-type fish, treatment with 75 μM 18β-glycyrrhetinic acid blocked the slow spontaneous synaptic currents and had no effect on the kinetics of the fast synaptic currents. At –90 mV, wild-type ($n = 14$) and *sho* ($n = 12$) fish exhibited identical values for both mean rise time (0.2 ± 0.1 ms) and mean decay time (0.6 ± 0.1 ms) of large spontaneous synaptic currents in fast muscle. The mean rise time for slow

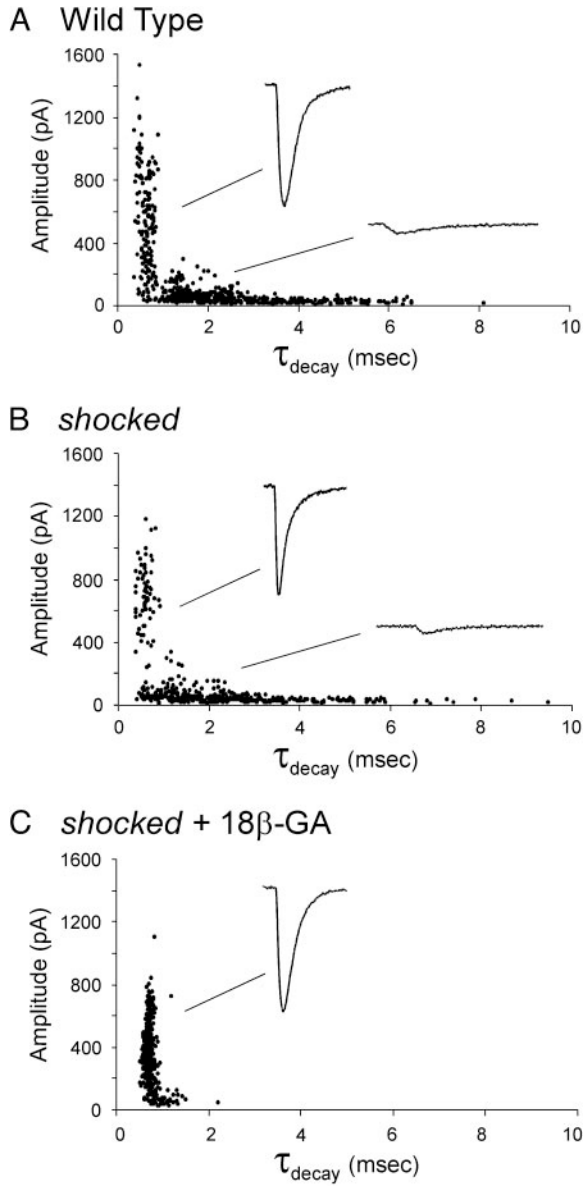

FIG. 3. Amplitude vs. decay scatter plots of synaptic currents from fast muscle cells of 3-day wild-type fish in *A* and 3-day *sho* fish in *B*. Each point represents a single spontaneous synaptic current. The decay time constant was determined by fit of the decay phase with a single-exponential function. Representative fast and slow synaptic currents are shown as *insets*. The scatterplots are composite recordings from 14 wild-type and 12 *sho* fast muscle cells. The synaptic currents were recorded in the presence of 1 μM TTX to block evoked responses. *C*: the effect of 75 μM 18β-glycyrrhetinic acid on spontaneous events for *sho*.

small events measured 0.8 ± 0.2 ms for both wild-type and *sho* fish. The mean decay time for slow small events measured 2.2 ± 0.6 ms in wild type; this was not significantly different from the 2.5 ± 0.8 ms obtained from *sho* recordings (P = 0.26). The fact that spontaneous synaptic current kinetics were similar in *sho* and wild-type fish pointed to differences in electrical coupling as causal to the differences in evoked synaptic responses rather than altered receptor kinetics.

To test for differences in electrical coupling, dual-muscle whole cell recordings were performed on *sho* fish at two time points of development. Early recordings at days 3 to 4 corresponded to the times at which *sho* fish were unable to mount an escape response (Fig. 1*A*). Subsequent recordings on day 6 fish corresponded to the time when some of the *sho* mutants had belatedly acquired the ability to mount an escape response (Fig. 1*A*). This window of improvement offered a unique opportunity to test for the potential involvement of electrical coupling in the *sho* phenotype.

On days 3–4, the coefficient of electrical coupling was determined for each cell pair for frequencies between 1 Hz and 6 kHz (Fig. 4*A*). For this purpose, sine wave command pulses were injected into one of the cells, and the magnitude of the follower current in the adjacent muscle was used to obtain the coupling coefficient. As found for other coupled networks, the coefficient was frequency dependent with the characteristics of a low-pass filter (Galarreta and Hestrin 1999). For slow skeletal muscle of wild-type fish, the mean network-coupling coefficient was 0.63 ± 0.08 (n = 5) at 1 Hz. The coupling measured for slow muscle of *sho* fish corresponded to 0.69 ± 0.08 (n = 6) and was not significantly different from wild-type fish (P = 0.29). Fast skeletal muscle of wild-type fish was weakly coupled with a mean network-coupling coefficient of 0.11 ± 0.07 (n = 7) at 1 Hz (Fig. 4*A*). By contrast, fast muscle in *sho* fish exhibited significant increases in network coupling at all frequencies tested (Fig. 4*A*). At 1 Hz, the coefficient was 0.32 ± 0.10 (n = 6) for *sho;* this was nearly three times greater than wild-type (P < 0.001). The high-frequency cutoff determined for *sho* fast muscle pairs (1.5 kHz) averaged nearly four times greater than wild-type (400 Hz) fast muscle pairs. This extension to higher frequency is probably not specific to *sho* muscle, but more likely results from the ability to resolve small current passage due to increased coupling. Previous studies have shown that fast muscle in larval zebrafish is dye coupled (Nguyen et al. 1999). Therefore we attempted to observe differences in dye coupling that would reflect the increased electrical coupling in *sho* fish. However, no significant differences (P = 0.84) in dye spread were observed between fast muscle of 3 day wild-type (3.3 ± 1.2; n = 8) and *sho* (3.4 ± 1.0; n = 9).

Next coupling coefficients were determined for the recovered pool of day 6 *sho* fish. The *sho* fish used for these experiments were initially screened at day 3 to determine that they exhibited the phenotype. They were screened again, just prior to recording, to ascertain that they had acquired the ability to mount an escape response. The coupling coefficient for day 6 *sho* fish corresponded to 0.12 ± 0.11 (n = 8), which is significantly lower than the 0.32 ± 0.10 value obtained for day 3 *sho* (P = 0.003) and not significantly different from that obtained for day 3–4 wild-type fish (P = 0.84).

Differences in electrical coupling between *sho* and wild-type fast muscle were further reflected in the ability of spontaneous synaptic currents to pass between muscle cells (Fig. 4*B*). In wild-type fish, the fast synaptic responses that appear on day 3 are no longer able to effectively pass to adjacent muscle preventing estimates of coupling coefficients. However, in *sho* fish, the largest spontaneous synaptic events generated in one cell consistently produced a much smaller and slower counterpart in the second muscle cell (Fig. 4*B*). The distortion and reduction in amplitude are consequences of the low-pass filtering by the network electrical properties. Additionally, very small events that were exceptionally slow were also seen occasionally in both muscle cells as paired events (data not shown). These small events were likely generated in a third cell

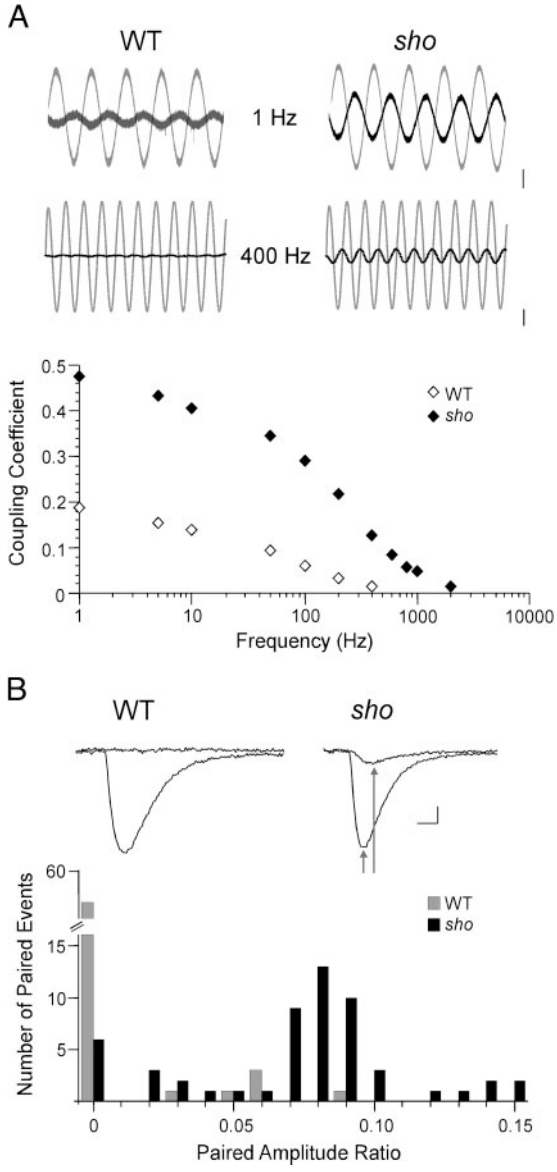

FIG. 4. Estimates of electrical coupling in fast skeletal muscle from dual voltage-clamp measurements of day 3 fish. *A*: sine wave command voltages were injected into fast muscle cells of wild-type (*left*) and *sho* (*right*) fish and the current responses recorded in adjacent muscle. *Top*: sample recordings of the current generated in each cell pair. The command current in the leader cell is shown in gray and the transcellular current in the follower cell is shown in black. The responses to low-frequency 1-Hz and high-frequency 400-Hz command sine waves are indicated. The histogram shows the coupling coefficients for a wild-type (◇) and a *sho* (◆) fast muscle over a range of frequencies. The 1-Hz calibration bar corresponds to 75 pA for WT and 100 pA for *sho*, and 400-Hz calibration bar corresponds to 200 pA in both WT and *sho*. *B*: the electrical coupling was estimated on the bases of the ratio of amplitudes for spontaneous synaptic pairs. Sample synaptic currents are shown for wild-type (*left*) and *sho* (*right*) paired voltage-clamp recordings. The vertical lines correspond to the peak for each synaptic current. The phase delay for this pair corresponded to 0.14 ms and the rise times measured 0.15 and 0.32 ms. The calibration bar corresponds to 100 pA and 400 μs. A frequency histogram of amplitude ratios for paired synaptic currents from wild-type (▨) and *sho* (■) fast muscle. Only events that were larger than 300 pA in 1 of the 2 cells were included and the ratio of peaks (smaller:larger event) was computed. In wild-type muscle, most of the synaptic currents showed no evidence of coupling. However, in each case the 2 cells were shown to be electrically coupled using the voltage protocol in *A*.

rather than either of the cells under voltage clamp. This conclusion is based on a paired amplitude ratio that is near unity and the lack of a phase shift between paired events, indicative of the fact that both events had traversed the low-frequency filter. These criteria were used to exclude such events from the estimates of coupling. An amplitude ratio histogram of the events was therefore based solely on events deemed to be generated in either of the two voltage-clamped muscle cells (Fig. 4*B*). Coupling coefficients, determined in this manner, could not be determined accurately for fast muscle of wild-type fish because the coupling was too weak and infrequent. However, the mean coupling ratio determined for *sho* fish on the basis of synaptic currents corresponded to 0.07 ± 0.04. The coupling ratio was lower than the coefficient determined with 1-Hz sine waves because of the low-pass characteristics of the network. Moreover, the frequency that provides coupling coefficients that were comparable to paired synaptic amplitude ratio was 400 Hz, reflecting the higher frequency components of the synaptic currents.

The primary candidate for mediation of electrical coupling between skeletal muscle cells is connexin 43 (Balogh et al. 1993). A role for connexin 43 in the *sho* phenotype was investigated by sequence analysis of genomic DNA obtained from mutant fish and by genetic mapping. No mutations in the coding sequence of connexin 43 were found. However, two neutral base pair polymorphisms were identified within individual *sho* mutants, indicating that recombination had occurred within the connexin 43 gene. Therefore this gene was not tightly linked to the *sho* mutation. Indeed results of our bulk segregant analysis revealed that the *sho* mutation maps to chromosome 2 (LG2). Current assembly information provided by the zebrafish genome sequencing project indicates that connexin 43 resides instead on chromosome 20 (LG20) (www.ensembl.org/Danio_rerio), ruling out the possibility of a mutation within the entire connexin 43 gene.

DISCUSSION

Our findings indicate that the timed loss of electrical coupling in fast skeletal muscle that occurs during early development may play an important role in coordinated movement. On initial formation of synapses, ACh receptor kinetics are slow, providing more effective depolarization of muscle (Jaramillo et al. 1988). We found that depolarization is also promoted through the network of electrically coupled muscle. Greater depolarizing drive is likely provided to those muscle cells with newly formed synapses via the temporal and spatial summation of stimulus evoked slow synaptic currents. During the course of fast muscle maturation, the kinetics of the synaptic current accelerate commensurate with a loss of electrical coupling (Buss and Drapeau 2000). This switch to fast synaptic kinetics, along with the newly acquired ability of fast muscle to generate spikes, provides for fast contractures and associated movements. It is this combination of developmental events that results in the acquisition of functional autonomy of fast muscle. Our findings from *sho* fish suggest that there are important negative consequences to delaying the developmental loss of electrical coupling in zebrafish, including the inability to effectively mount a sustained series of fast contractions.

At the developmental stages where *sho* fish exhibited aborted escape responses, our measurements of electrical cou-

pling revealed a threefold elevation over wild-type fish. Generally, in wild-type fish, the fast muscle was functionally uncoupled so that even the very largest synaptic currents failed to spread to the neighboring cell. In *sho* fish, however, the increased electrical coupling was manifest as an ability of large synaptic currents, both evoked and spontaneous, to effectively transit the gap junctions. Importantly, the shared electrotonic reflections were even larger for evoked than spontaneous currents. This is due to the fact that evoked currents were frequently very large (>10 nA) at the site of origin, reflecting the nearly synchronous release of multiple quanta. Additionally, many such responses contribute to the overall electrotonic reflection because each motor neuron innervates a large field of electrically coupled muscle cells thereby producing significant strengthening of responses as reflected in our current-clamp measurements. Finally, the kinetics of electrotonically transmitted currents were slowed by the network filtering (Galarreta and Hestrin 1999), producing an even more effective depolarization of neighboring muscle. The slowed electrotonic inward current was manifest as an afterdepolarization in the neighboring muscle. Such afterdepolarizations were also observed in some wild-type recordings because fast muscle was still weakly coupled at this stage of development. However, both the amplitudes and decay times were significantly less when compared with *sho* at a comparable age. Finally, it is important to point out that the excessive electrical coupling will result in altered time constants of muscle membrane depolarization that may directly contribute to the shape of the action potential. It is difficult to sort out the relative contributions from shared synaptic current versus altered input resistance. However, the fact that we see differences in the evoked current under voltage clamp indicates that the electrotonic currents are likely to contribute significantly to the depolarization in *sho* fish.

The fact that *sho* fish appeared to be less touch-sensitive, in addition to the swimming dysfunction, makes it likely that factors other than excessive electrical coupling in muscle contribute to the phenotype. Additionally, the mutant fish died within the first 2 wk after birth despite the improved ability to swim. Thus there is clearly an additional manifestation of the mutation rendering the effects on muscle electrical coupling as secondary. However, our analyses of synaptic function suggest that excessive electrical coupling in *sho* fish contributes to the single-tail-flip phenotype. Indeed, our data support the idea that the aforementioned slow component of evoked current seen in *sho* could potentially account for this characteristic of the phenotype. The slow component of inward current in *sho* fish results in an exaggerated and prolonged afterdepolarization after stimulation of the motor nerve. The prolonged afterdepolarization would be expected to increase both the strength and duration of muscle contraction. Our high-speed analyses of escape responses in *sho* fish at day 3 are consistent with the idea that the initial bend is prolonged compared with wild type. In some types of vertebrate skeletal muscle, such a prolongation may not impact on muscle contraction speed. However, skeletal muscle in zebrafish has exceedingly fast contraction as reflected in the swimming responses shown in Fig. 1. The wave of swimming activity in zebrafish occurs at ~20 Hz and can achieve speeds as high as 70 Hz (Masino and Fetcho 2003). The two- to threefold prolongation of depolarization in *sho* could potentially lead to physical interference of fast contraction or alternatively might interfere with the ability to generate muscle action potentials. Further support for the idea that excessive electrical coupling underlies the abortive swimming was provided by recordings from 6-day-old *sho* fish. At this stage of development, many of the mutant fish have recovered to the extent that they can mount reasonable escape responses. The measurements of network coupling in these fish indicate coefficients that have decreased to a level commensurate with day 3 wild-type fish, the stage at which wild-type fish acquire the ability to mount an effective escape response. Thus like *Xenopus,* zebrafish appear to undergo a reduction in electrical coupling of fast muscle during early development (Armstrong et al. 1983). Finally, recordings from ventral roots of motor neurons indicate that patterned output can occur in *sho* fish. Like wild-type fish we observe long episodes of motor neuron bursting that normally drives swimming behavior. However, *sho* is unable to exhibit such swimming, further indicating that part of the problem lies in the ability of muscle to follow the CNS drive. Because the fish were paralyzed with α-bungarotoxin it is possible that muscle contractions in *sho* normally alter the motor output through some type of feedback. However, we were unable to test the idea because of the large movements associated with fictive swimming in nonparalyzed fish. Overall, these findings suggest that this timed loss of electrical coupling in muscle plays an important role in the acquisition of the fast movements such as those involved in escape responses.

The locus of the *sho* mutation is not known, precluding direct tests for a role of electrical coupling in conferring the phenotype. Connexin 43 is the principle subunit of gap junctions expressed in skeletal muscle (Balogh et al. 1993), but our results rule out a mutation in this gene as causal to the phenotype. Sequencing the coding region of *sho* connexin 43 revealed no mutations, and mapping the *sho* locus to LG2 appears to eliminate connexin 43 as a candidate. According to current data provided by the genome sequencing project (www.ensembl.org/Danio_rerio), connexin 43 resides on LG20. Thus the mechanisms causal to the increased electrical coupling of *sho* resides in a mutation involving either another connexin gene or, alternatively, in a gene the product of which can affect electrical coupling. A gene other than connexin is further suggested by the fact that *sho* fish exhibit a higher threshold for escape response and eventually die despite the eventual loss of excessive electrical coupling. Ultimately, the solution to this interesting problem will await identification of the genetic mutation underlying the *sho* phenotype.

ACKNOWLEDGMENTS

We thank Drs. Masino, McLean and Fetcho for advice on ventral root recordings. Dr. Frohnhoefer (Max-Planck-Institute, Tuebingen, Germany) provided mutant *shocked* zebrafish. R. Grady provided expert maintenance of the fish colony.

Present address of F. Ono: Whitney Laboratory, University of Florida, St. Augustine, FL 32080-8610.

GRANTS

This study was supported by National Institute of Neurological Disorders and Stroke Grants NS-18205 and NS-045935 to P. Brehm. G. Mandel is an Investigator of the Howard Hughes Medical Institute.

REFERENCES

Armstrong DL, Turin L, and Warner AE. Muscle activity and the loss of electrical coupling between striated muscle cells in *Xenopus* embryos. *J Neurosci* 3: 1414–1421, 1983.

Balogh S, Naus C, and Merrifield PA. Expression of gap junctions in cultured rat L6 cells during myogenesis. *Dev Biol* 155: 351–360, 1993.

Brehm P and Henderson L. Regulation of acetylcholine receptor channel function during development of skeletal muscle. *Dev Biol* 129: 1–11, 1988.

Brehm P, Kullberg R, and Moody-Corbett F. Properties of nonjunctional acetylcholine receptor channels on innervated muscle of *Xenopus laevis*. *J Physiol* 350: 631–648, 1984.

Buss R and Drapeau P. Physiological properties of zebrafish embryonic red and white muscle fibers during early development. *J Neurophysiol* 84: 1545–1557, 2000.

Galarreta M and Hestrin S. A network of fast-spiking cells in the neocortex connected by electrical synapses. *Nature* 402: 72–75, 1999.

Granato M, van Eeden FJ, Schach U, Trowe T, Brand M, Furutani-Seiki M, Haffter P, Hammerschmidt M, Heisenberg CP, Jiang YJ, Kane DA, Kelsh RN, Mullins MC, Odenthal J, and Nusslein-Volhard C. Genes controlling and mediating locomotion behavior of the zebrafish embryo and larva. *Development* 123: 399–413, 1996.

Harris A. Emerging issues of connexin channels: biophysics fills the gap. *Q Rev Biophys* 34: 325–472, 2001.

Jaramillo F, Vicini S, and Schuetze SM. Embryonic acetylcholine receptors guarantee spontaneous contractions in rat developing muscle. *Nature* 335: 66–68, 1988.

Lefebvre JL, Ono F, Puglielli C, Saidner G, Franzini-Armstrong C, Brehm P, and Granato M. Increased neuromuscular activity causes axonal defects and muscle degeneration. *Development* 131: 2605–2618, 2004.

Masino M and Fetcho J. Fictive swimming motor patterns in wildtype and mutant larval zebrafish. *Soc Neurosci Abstr* 277.2, 2003.

Nguyen PV, Aniksztejn L, Catarsi S, and Drapeau P. Maturation of neuromuscular transmission during early development in zebrafish. *J Neurophysiol* 81: 2852–2861, 1999.

Ono F, Higashijima S, Shcherbatko A, Fetcho J, and Brehm P. Paralytic zebrafish lacking acetylcholine receptors fail to localize rapsyn clusters to the synapse. *J Neurosci* 21: 5439–5448, 2001.

Ono F, Shcherbatko A, Higashijima S, Mandel G, and Brehm P. The zebrafish motility mutant twitch once reveals new roles for rapsyn in synaptic function. *J Neurosci* 22: 6491–6498, 2002.

Postlethwait JH and Talbot WS. Zebrafish genomics: from mutants to genes. *Trends Genet* 13: 183–190, 1997.

Proulx A, Merrifield P, and Naus C. Blocking gap junctional intercellular communication in myoblasts inhibits myogenin and MRF4 expression. *Dev Genet* 20: 133–144, 1997.

Schmalbruch H. Skeletal muscle fibers of newborn rats are coupled by gap junctions. *Dev Biol* 91: 485–490, 1982.